Phys. Status Solidi B **253,** No. 8, 1638–1642 (2016) / **DOI** 10.1002/pssb.201600058

physica status solidi b
www.pss-b.com
basic solid state physics

Bogoliubov–de Gennes study of nanoscale Hubbard superconductors

César G. Galván[1], José M. Cabrera-Trujillo[1], Luis A. Pérez[2], and Chumin Wang[*,3]

[1] Facultad de Ciencias, Universidad Autónoma de San Luis Potosí, S.L.P., Mexico
[2] Instituto de Física, Universidad Nacional Autónoma de México, A.P. 20-364, 01000 Mexico City, Mexico
[3] Instituto de Investigaciones en Materiales, Universidad Nacional Autónoma de México, A.P. 70-360, 04510 Mexico City, Mexico

Received 1 February 2016, revised 1 April 2016, accepted 4 April 2016
Published online 28 April 2016

Keywords Bogoliubov–de Gennes formalism, grains, Hubbard model, superconductivity

[*] Corresponding author: e-mail chumin@unam.mx, Phone: +52-55-56224634, Fax: +52-55-56161251

The effects of quantum confinement on the superconducting ground state are studied within the Bogoliubov–de Gennes (BdG) formalism and an attractive Hubbard model. We consider a periodic arrangement of two-dimensional superconducting grains composed by $N \times N$ atoms surrounded by insulating, metallic or superconducting stripes with a thickness of s atoms, leading to $2(N+s)^2$ coupled self-consistent BdG equations for a supercell of $(N+s) \times (N+s)$ atoms. These equations determine the spatial variation of superconducting gap as functions of temperature, electron–electron interaction, and hopping integrals analyzing three types of boundary stripes. The results show a clear enhancement of the superconducting gap and critical temperature induced by the electron confinement in the grain, being larger for the insulating boundary case. Finally, the numerical solutions of BdG equations are compared with those obtained by applying the BCS theory to each grain site.

1 Introduction Quantum confinement can significantly modify many physical properties of a material, such as enhancements of semiconducting band gap [1] and ferromagnetic moments [2]. In 1959, P. W. Anderson found that superconductivity persists in single grains if their average energy-level separation is smaller than the bulk superconducting gap [3]. Moreover, in an array of superconducting grains separated by normal material interfaces, there is an inter-grain coupling due to the proximity effect, where the superconducting wave function varies smoothly across the interface causing a suppression of the pair amplitude in the superconductor and an enhancement of superconductivity in the normal side. Moreover, if the width of these interfaces is thin enough, the superconducting phases in neighboring grains are locked, as occurred in the Josephson junctions [4].

On the theoretical side, the Bogoliubov–de Gennes formalism [5] provides a real-space description of superconducting properties. Furthermore, the attractive Hubbard model emphasizes local electron–electron interactions and has been used to investigate high-T_c superconductivity, where the dynamics of charge carriers can be described by a single-band square-lattice Hubbard model [6]. Moreover, most of high-T_c ceramic superconductors are polycrystalline structures composed by superconducting grains [7]. In this article, we report a detailed study of quantum confinement and boundary coupling effects on grain superconductors by solving the Bogoliubov–de Gennes self-consistent equations. This study was carried out by using the supercell technique, which leads to $2(N+s)^2$ coupled equations for a square-lattice supercell of $(N+s) \times (N+s)$ atoms. The self-consistent solution of these equations gives the local superconducting gaps that depend on the grain size and boundary nature, which can be insulator, metal, or superconductor.

2 The model Let us consider a square lattice supercell of $(N+s) \times (N+s)$ atoms consisting of a superconducting grain represented by $N \times N$ A-type atoms bordered by $(2N+s)s$ B-type ones, described by a single-band attractive Hubbard Hamiltonian [6, 8] given by

$$\hat{H} = \sum_{l,\sigma} \varepsilon_l \hat{n}_{l,\sigma} + \sum_{\langle l,m\rangle,\sigma} t_{l,m} \hat{c}^{\dagger}_{l,\sigma} \hat{c}_{m,\sigma} + \sum_{l} U_l \hat{n}_{l,\uparrow} \hat{n}_{l,\downarrow}, \qquad (1)$$

where $\hat{c}^{\dagger}_{l,\sigma}$ ($\hat{c}_{l,\sigma}$) is the creation (annihilation) operator with spin $\sigma = \uparrow$ or $\downarrow$ at site l, $\hat{n}_{l,\sigma} = \hat{c}^{\dagger}_{l,\sigma} \hat{c}_{l,\sigma}$, and $\langle l, m\rangle$ denotes

nearest neighbor sites. In the supercell, A- and B-type atoms, respectively, have on-site energies ε_A and ε_B, and the hopping integrals between these atoms could be t_{AA}, t_{AB}, or t_{BB}. Moreover, the on-site electron–electron interactions are U_A and U_B, respectively, for A- and B-type atoms.

Hamiltonian (1) in the mean-field approximation can be rewritten as

$$\hat{H}_{MF} = \varepsilon_0 + \sum_{l,\sigma} \tilde{\varepsilon}_l \hat{n}_{l,\sigma} + \sum_{\langle l,m\rangle,\sigma} t_{l,m} \hat{c}^{\dagger}_{l,\sigma} \hat{c}_{m,\sigma} + \sum_{l} (\Lambda^{*}_{l,l} \hat{c}_{l,\downarrow} \hat{c}_{l,\uparrow} + \Lambda_{l,l} \hat{c}^{\dagger}_{l,\uparrow} \hat{c}^{\dagger}_{l,\downarrow}), \quad (2)$$

where $\varepsilon_0 = -\sum_l U_l \rho_l^2/4$, $\tilde{\varepsilon}_l = \varepsilon_l + U_l \rho_l/2$, and $\Lambda_{l,l} = U_l \langle \hat{c}_{l,\downarrow} \hat{c}_{l,\uparrow} \rangle$, being $\rho_l = \langle \hat{n}_{l,\uparrow} \rangle + \langle \hat{n}_{l,\downarrow} \rangle$ the electron density at atom l and $\langle \hat{n}_{l,\uparrow} \rangle = \langle \hat{n}_{l,\downarrow} \rangle$ for non-spin-polarized materials.

Applying the unitary transformation [5]

$$\hat{c}_{l,\uparrow} = \sum_{\alpha} \left(u^{\alpha}_{l} \hat{\gamma}_{\alpha,\uparrow} - v^{\alpha *}_{l} \hat{\gamma}^{\dagger}_{\alpha,\downarrow} \right) \text{ and } \hat{c}_{l,\downarrow} = \sum_{\alpha} \left(u^{\alpha}_{l} \hat{\gamma}_{\alpha,\downarrow} + v^{\alpha *}_{l} \hat{\gamma}^{\dagger}_{\alpha,\uparrow} \right), \quad (3)$$

to $\hat{H}_{MF} - \mu \hat{N}$ with μ the chemical potential and $\hat{N} = \sum_{l,\sigma} \hat{n}_{l,\sigma}$, and using the supercell technique by rewriting

$$\begin{pmatrix} u^{\alpha}_{l} \\ v^{\alpha}_{l} \end{pmatrix} \Rightarrow e^{i\mathbf{k}\cdot\mathbf{r}_l} \begin{pmatrix} u^{\alpha}_{l}(\mathbf{k}) \\ v^{\alpha}_{l}(\mathbf{k}) \end{pmatrix}, \quad (4)$$

the Bogoliubov–de Gennes equations for $u^{\alpha}_{l}(\mathbf{k})$ and $v^{\alpha}_{l}(\mathbf{k})$ are [5]

$$\sum_{m} e^{i\mathbf{k}\cdot(\mathbf{r}_m - \mathbf{r}_l)} \begin{pmatrix} H_{l,m} & \Lambda_{l,m} \\ \Lambda^{*}_{l,m} & -H^{*}_{l,m} \end{pmatrix} \begin{pmatrix} u^{\alpha}_{m}(\mathbf{k}) \\ v^{\alpha}_{m}(\mathbf{k}) \end{pmatrix} = E^{\alpha}(\mathbf{k}) \begin{pmatrix} u^{\alpha}_{l}(\mathbf{k}) \\ v^{\alpha}_{l}(\mathbf{k}) \end{pmatrix}, \quad (5)$$

where $H_{l,m} = (\tilde{\varepsilon}_l - \mu)\delta_{l,m} + t_{l,m}\Theta_{l,m}$ and

$$\Lambda_{l,m} = -\frac{U_l}{2} \delta_{l,m} \sum_{\alpha,\mathbf{k}} \begin{bmatrix} u^{\alpha}_{l}(\mathbf{k}) v^{\alpha *}_{m}(\mathbf{k}) e^{-i\mathbf{k}\cdot(\mathbf{r}_m - \mathbf{r}_l)} \\ + u^{\alpha}_{m}(\mathbf{k}) v^{\alpha *}_{l}(\mathbf{k}) e^{i\mathbf{k}\cdot(\mathbf{r}_m - \mathbf{r}_l)} \end{bmatrix} \tanh \frac{E^{\alpha}(\mathbf{k})}{2k_B T}, \quad (6)$$

being

$$\Theta_{l,m} = \begin{cases} 1, \text{ if } l \text{ and } m \text{ are nearest neighbors} \\ 0, \text{ other cases.} \end{cases} \quad (7)$$

Assuming a uniform initial distribution of $\Lambda_{l,m}$, the eigenvalue Eq. (5) is solved to determine $E^{\alpha}(\mathbf{k})$, $u^{\alpha}_{l}(\mathbf{k})$, and $v^{\alpha}_{l}(\mathbf{k})$, which are substituted into Eq. (6) to get a new $\Lambda_{l,m}$. This procedure is repeated until a relative convergence of 10^{-4} is achieved, obtaining the superconducting gaps ($\Delta_l = \Lambda_{l,l}$) for each site l.

3 Results Starting from a homogeneous gap seed, Eq. (5) is self-consistently solved for Δ_l induced by an attractive on-site electron–electron interaction $U_A = -0.5t$ with hopping integrals $t_{AA} = -t < 0$. Figure 1(a–c) shows the spatial variation of superconducting gap Δ_l for a superconducting grain composed of A-type atoms with $N = 8$, $s = 1$, $\rho_A = \rho_B = 1$, $\varepsilon_A = 0$, $\varepsilon_B = (U_A - U_B)/2$ and surrounded by (a) a weaker superconductor with $U_B = 0.5U_A$ and $t_{AB} = t_{BB} = t_{AA}$; (b) a normal metal with $U_B = 0$ and $t_{AB} = t_{BB} = t_{AA}$; and (c) an insulator with $t_{AB} = t_{BB} = U_B = 0$. Figure 1(a′–c′) corresponds to systems with the same parameters as in Fig. 1(a–c), except for $s = 2$. Observe that $\Delta_{l\in A}$ in case (a) are larger than those in (b), where the extreme values of gap for case (a) are $\Delta^{max}_{l\in A} = 0.00248t$ and $\Delta^{min}_{l\in A} = 0.00232t$, whereas $\Delta^{max}_{l\in A} = 0.00227t$ and $\Delta^{min}_{l\in A} = 0.00211t$ for case (b). Furthermore, when the grain-boundary width increases, $\Delta_{l\in A}$ diminish and the superconducting-gap variation augments in the grain, as observed in Fig. 1(a′–c′) in comparison to the corresponding Fig. 1(a–c). The extreme gap values for case (a′) are $\Delta^{max}_{l\in A} = 0.00248t$ and $\Delta^{min}_{l\in A} = 0.00232t$, whereas $\Delta^{max}_{l\in A} = 0.00227t$ and $\Delta^{min}_{l\in A} = 0.00211t$ for case (b′). These trends are consistent with the superconducting proximity effect [4].

Figure 1(c and c′), respectively, illustrate the superconducting gap ($\Delta_{l\in A}$) distribution for $s = 1$ and $s = 2$, when the grain is surrounded by an insulator with $t_{AB} = t_{BB} = U_B = 0$. Note the significant larger values of $\Delta_{l\in A}$ along the diagonal sites (red bars) forming a cross. This fact could be related to the inhomogeneity of the single-electron local density of states (LDOS), which can be calculated using the convolution theorem [9], since the

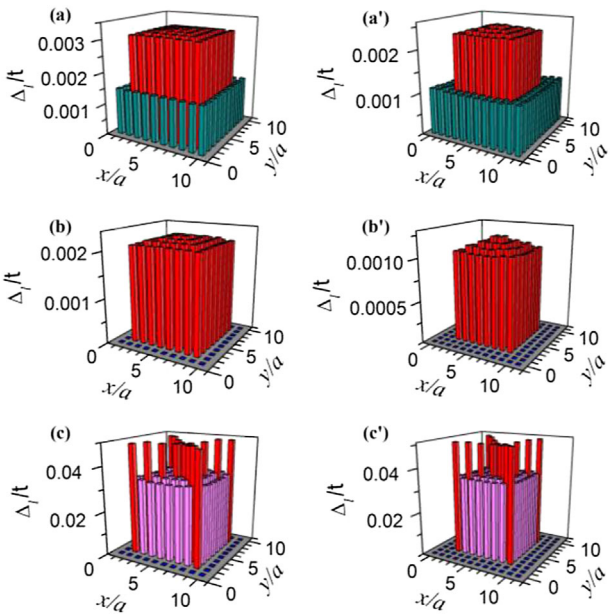

Figure 1 Local superconducting gap (Δ_l) in a square-lattice supercell with 8×8 A-type atoms surrounded by (a–c) single and (a′–c′) double line stripes of B-type atoms, which can be (a,a′) a weaker superconductor, (b,b′) a normal metal, or (c,c′) an insulator.

single-electron tight-binding Hamiltonian is separable, given by

$$\mathrm{LDOS}^{2\mathrm{D}}_{(x,y)}(E) = \int_{-\infty}^{\infty} \mathrm{d}\xi\, \mathrm{LDOS}^{1\mathrm{D}}_{x}(E-\xi)\mathrm{LDOS}^{1\mathrm{D}}_{y}(\xi), \tag{8}$$

where the one-dimensional LDOS [10] is

$$\mathrm{LDOS}^{1\mathrm{D}}_{x}(E) = -\frac{1}{\pi}\lim_{\eta\to 0^{+}} \mathrm{Im}\sum_{n=1}^{N}\frac{\langle x|n\rangle\langle n|x\rangle}{E-E_n+i\eta}, \tag{9}$$

with

$$\langle x|n\rangle = \sqrt{\frac{2}{N+1}}\sin\frac{n\pi x}{(N+1)a} \tag{10}$$

and

$$E_n = \varepsilon_{\mathrm{A}} + 2t_{\mathrm{AA}}\cos\frac{n\pi}{N+1} \tag{11}$$

for a linear chain of N atoms with lattice parameter a [11]. For the case of a half-filling band, the chemical potential is located at a van Hove singularity ($\mu = \varepsilon_{\mathrm{A}}$) and from Eqs. (8–11) we obtain a relationship between the LDOS of diagonal ($|x| = |y|$) and non-diagonal ($|x| \neq |y|$) sites given by

$$\mathrm{LDOS}^{2\mathrm{D}}_{|x|\neq|y|}(\varepsilon_{\mathrm{A}}) \cong \frac{2}{3}\mathrm{LDOS}^{2\mathrm{D}}_{|x|=|y|}(\varepsilon_{\mathrm{A}}), \tag{12}$$

whose specific values depend on the imaginary part of energy (η) used.

Now, for an attractive Hubbard model (1), the superconducting gap (Δ) at $T = 0\,\mathrm{K}$ is determined by the BCS equation [6, 12] given by

$$\begin{aligned} 1 &= \frac{-U}{2N_S}\sum_{\mathbf{k}}\frac{1}{\sqrt{[\varepsilon(\mathbf{k})-\mu]^2+\Delta^2}} \\ &= -\frac{U}{2}\int_{-4t}^{4t}\frac{\mathrm{DOS}(\varepsilon)\mathrm{d}\varepsilon}{\sqrt{[\varepsilon-\mu]^2+\Delta^2}}, \end{aligned} \tag{13}$$

where N_S, $\varepsilon(\mathbf{k})$, and $\mathrm{DOS}(\varepsilon)$ are, respectively, the total number of atoms, the dispersion relation, and single-electron density of states of a homogeneous square lattice with null self-energy and nearest-neighbor hopping integral $-t$. This density of states can be approximated by

$$\mathrm{DOS}(\varepsilon) \approx \begin{cases} D + F\delta(\varepsilon), & \text{if } |\varepsilon| \leq 4t \\ 0, & \text{if } |\varepsilon| > 4t, \end{cases} \tag{14}$$

where $\delta(\varepsilon)$ is the Dirac delta function that mimics the van Hove singularity. The condition $\int_{-4t}^{4t}\mathrm{DOS}(\varepsilon)\mathrm{d}\varepsilon = 1$ leads to

$$F = 1 - 8tD. \tag{15}$$

For the case of a half-filling band ($\mu = 0$), substituting Eqs. (14) and (15) into Eq. (13) we obtain

$$\begin{aligned} 1 &= |U|D\sinh^{-1}\left(\frac{4t}{\Delta}\right) + \frac{|U|F}{2\Delta} \\ &= |U|\frac{1-F}{8t}\sinh^{-1}\left(\frac{4t}{\Delta}\right) + \frac{|U|F}{2\Delta}. \end{aligned} \tag{16}$$

If we assume that Eq. (16) is satisfied for each site in the studied finite square lattice, the local superconducting gap at diagonal (Δ_{d}) and non-diagonal (Δ_{nd}) A-type sites in Fig. 1 (c and c′) are related by $\Delta_{\mathrm{d}} \approx 1.3906\Delta_{\mathrm{nd}}$, as Eq. (12) leads to $F_{\mathrm{d}} \cong \frac{3}{2}F_{\mathrm{nd}}$ and we apply Eq. (16) to both diagonal and non-diagonal sites. This relation describes the main features of Fig. 1(c and c′) with a relative standard deviation of 4% and 3%, respectively, where Δ_{d} has been taken as the maximum local superconducting gap obtained from the Bogoliubov–de Gennes formalism.

Figure 2 shows the average superconducting gap over A-type atoms ($\langle\Delta_{l\in\mathrm{A}}\rangle$) as a function of the hopping integral at the B-type boundary zone ($t_{\mathrm{B}} = t_{\mathrm{AB}} = t_{\mathrm{BB}}$) for the same systems of Fig. 1 with single ($s = 1$) and double ($s = 2$) line boundaries.

Observe a more than 10 times increment of $\langle\Delta_{l\in\mathrm{A}}\rangle$ when t_{B} diminishes from $t_{\mathrm{B}} = t_{\mathrm{A}}$ to $t_{\mathrm{B}} = 0$, which suggests an enhancement of electron pairing induced by the single electron confinement in the grain (A-region) leading to a strong superconducting state. Furthermore, notice that

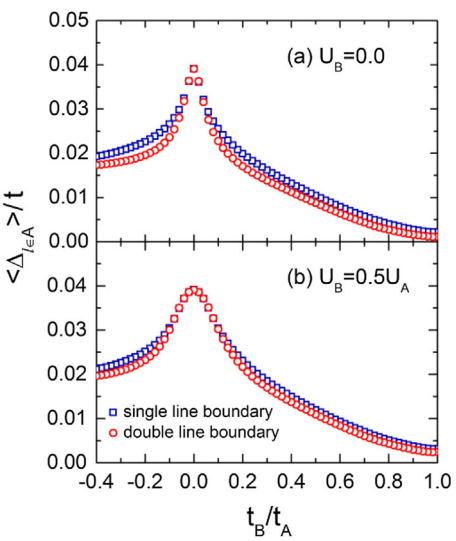

Figure 2 Average superconducting gap over A-type atoms ($\langle\Delta_{l\in\mathrm{A}}\rangle$) versus the hopping integral in the B-type boundary zone (t_{B}) for the same systems of Fig. 1 with (a) $U_{\mathrm{B}} = 0$ and (b) $U_{\mathrm{B}} = 0.5U_{\mathrm{A}}$.

$\langle\Delta_{l\in A}\rangle$ is larger for the single-line boundary case in comparison with those corresponding to the double-line case, as expected from the proximity effect. However, for t_B=0, $\langle\Delta_{l\in A}\rangle$ has the same value for both single- and double-line boundary cases, because the grains are disconnected from each other. In addition, note the asymmetry between negative and positive values of t_B. In particular, when $t_B/t_A < 0$, the superconducting states in A- and B-regions are, respectively, based on bonding and antibonding single-electron states, which could induce a confinement due to dephasing and then a more robust superconducting state is found at the $t_B/t_A < 0$ side.

In Fig. 3, the critical temperature (T_c) is plotted as a function of the grain side length (N) for systems with a single line boundary, U_A=$-0.5t$, $U_B = 0$, $t_A = -t$, $t_B = 0$, $0.1t$, $0.2t$, and $0.3t$. The inset of Fig. 3 illustrates the variation of $\langle\Delta_{l\in A}\rangle$ versus temperature (T) for 8×8 atom grains of Fig. 1 with $s = 1$. The critical temperatures were determined by the condition $\langle\Delta_{l\in A}\rangle = 0$. Observe that $\langle\Delta_{l\in A}\rangle$ has a BCS-like temperature variation for all analyzed cases. Moreover, T_c monotonically increases with the diminution of superconducting grain size when $t_B = 0$, and for $t_B \neq 0$ there is an optimum value of N where $T_c(N)$ reaches its maximum value. In fact, the increment of $T_c(N)$ with the diminution of grain size has been reported in aluminum [13], indium [13], and tin [14] granular superconductors. In addition, for a given grain size, T_c decreases when t_B grows, as expected from the proximity effect [4].

Finally, it would be worth mentioning that the bulk coherence length (ξ_0) at $T = 0$ can be calculated from Ref. [15]

$$\xi_0 = \frac{2\sqrt{2}}{\pi}\langle R^2\rangle^{1/2} = \frac{2\sqrt{2}}{\pi}\left[\frac{\sum_{\mathbf{R}} f^*(\mathbf{R})R^2 f(\mathbf{R})}{\sum_{\mathbf{R}} f^*(\mathbf{R}) f(\mathbf{R})}\right]^{1/2}, \quad (17)$$

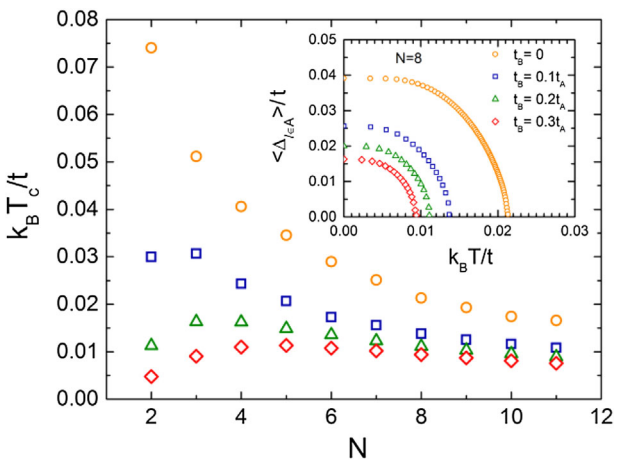

Figure 3 Critical temperature (T_c) versus the grain side length (N) for systems with a single line boundary. Inset: average superconducting gap over A-type atoms ($\langle\Delta_{l\in A}\rangle$) as a function of temperature (T) for the same systems of Fig. 1.

where $f(\mathbf{R})$=$\langle\hat{c}_{\mathbf{R}\downarrow}\hat{c}_{0\uparrow}\rangle/\langle\hat{c}_{0\downarrow}\hat{c}_{0\uparrow}\rangle$ with

$$\langle\hat{c}_{\mathbf{R}\downarrow}\hat{c}_{0\uparrow}\rangle = \frac{1}{N}\sum_{\mathbf{k}}\frac{\Delta}{2\sqrt{[\varepsilon(\mathbf{k})-\mu]^2+\Delta^2}}e^{i\mathbf{k}\cdot\mathbf{R}}. \quad (18)$$

For $U = -0.5t$, the bulk superconducting gap is $\Delta \simeq 0.00443t$ and then Eq. (17) leads to $\xi_0 \simeq 100.4a$. The supercell size was chosen to be smaller than ξ_0, in order to emphasize the quantum confinement effects. In fact, observe in Fig. 3 the almost constant value of T_c for different boundary conditions when N approaches to ξ_0.

4 Conclusions We have studied the finite grain size and boundary effects on the superconducting ground state by solving the Bogoliubov–de Gennes self-consistent equations for a square-lattice supercell described by an attractive Hubbard model. Three types of boundaries were considered, being insulator, normal conductor, and weak superconductor. The latter possesses smaller local superconducting gaps than those of the grain due to a weaker attractive electron–electron interaction. For all analyzed boundaries, the averaged superconducting gap over the grain sites ($\langle\Delta_{l\in A}\rangle$) can be larger than that of the corresponding bulk case for a small enough t_B. In particular, for the insulating boundary we found a significant enhancement of $\Delta_{l\in A}$, whose maximum values have a cross pattern in the square grain with a half-filled single electron band. This pattern can be reproduced with a less than 5% error by applying the Hubbard-BCS results to each site of the grain. On the other hand, the enhancement of both $\langle\Delta_{l\in A}\rangle$ and the critical temperature (T_c) could be related to the confinement of single-electron wave functions in the grain, which favors the electron pairing and the coherent state formation. For the normal-conductor boundary case, we observe an asymmetry in $\langle\Delta_{l\in A}\rangle$ when such conductor has an electron- or hole-type transport, being larger when the grain and its boundary have different types of charge carriers. Moreover, in this case the increase of T_c with the diminution of grain size is followed by a decay, which can be understood by the Anderson argument [3] and its further generalization for systems with energy-level degenerations [16]. It is important to emphasize that the electron pairing through attractive Hubbard model occurs over all the occupied electron states, in contrast to the thin energy shell of BCS theory [17]. In summary, the numerical solution of the Bogoliubov–de Gennes equations for attractive Hubbard model confirms the experimentally observed growth of T_c with the decrease of superconducting grain size and it can be qualitatively reproduced for the first time, to our knowledge, by applying the BCS superconducting gap formula to each site, whose pairing interaction was taken as the negative U of Hubbard model.

Acknowledgements This work has been partially supported by UNAM-PAPIIT-IN106714 and UNAM-PAPIIT-IN113714. C.G.G. recognizes the CONACyT postdoctoral

fellowship. L.A.P. acknowledges partial support from "Cátedra Marcos Moshinsky". Computations were performed at Miztli of DGTIC-UNAM.

References

[1] L. Canham (Ed.), Handbook of Porous Silicon (Springer, Switzerland, 2014).
[2] S. N. Khanna and A. W. Castleman (Eds.), Quantum Phenomena in Clusters and Nanostructures (Springer, Berlin, 2003).
[3] P. W. Anderson, J. Phys. Chem. Solids **11**, 26 (1959).
[4] A. Frydman and R. C. Dynes, Philos. Mag. B **81**, 1153 (2001).
[5] P. G. de Gennes, Superconductivity of Metals and Alloys (Addison-Wesley Publ. Co., New York, 1989).
[6] R. Micnas, J. Ranninger, and S. Robaszkiewicz, Rev. Mod. Phys. **62**, 113 (1990).
[7] S. E. Babcock and J. L. Vargas, Annu. Rev. Mater. Sci. **25**, 193 (1995).
[8] L. A. Pérez, C. G. Galván, and C. Wang, J. Supercond. Nov. Magn. **29**, 285 (2016).
[9] V. Sánchez and C. Wang, Phys. Rev. B **70**, 144807 (2004).
[10] E. N. Economou, Green's Functions in Quantum Physics (Springer, Berlin, 2006).
[11] A. P. Sutton, Electronic Structure of Materials (Clarendon Press, Oxford, 1993).
[12] L. A. Pérez, J. S. Millán, and C. Wang, Int. J. Mod. Phys. B **24**, 5229 (2010).
[13] S. Matsuo, H. Sugiura, and S. Noguchi, J. Low-Temp. Phys. **15**, 481 (1974).
[14] W.-H. Li, C.-W. Wang, C.-Y. Li, C. K. Hsu, C. C. Yang, and C.-M. Wu, Phys. Rev. B **77**, 094508 (2008).
[15] F. Marsiglio and J. E. Hirsch, Phys. Rev. B **41**, 6435 (1990).
[16] V. Z. Kresin and Y. N. Ovchinnikov, Phys. Usp. **51**, 427 (2008).
[17] J. Bardeen, L. N. Cooper, and J. R. Schrieffer, Phys. Rev. **108**, 1175 (1957).

